Distributed Genetic Algorithm for Subtraction Radiography

Gabriel Mañana
Universidad Nacional de Colombia
Centro de Telemedicina, Facultad de Medicina
Bogotá, Colombia
gjmananag@unal.edu.co

Fabio González
Universidad Nacional de Colombia
Laboratorio de Investigación en Sistemas Inteligentes
Bogotá, Colombia
fagonzalezo@unal.edu.co

Eduardo Romero
Universidad Nacional de Colombia
Centro de Telemedicina, Facultad de Medicina
Bogotá, Colombia
edromero@unal.edu.co

ABSTRACT

Digital subtraction is a promising technique used in radiographic studies of periapical lesions and other dental disorders for which the treatment must be evaluated over time. This paper presents a fast and reliable automated image registration method for subtracting two digitized radiographs where an unpredicted mismatch is present. An optimal affine transformation is found using an adaptive Genetic Algorithm (GA) as the optimization strategy and a correlation ratio as the similarity measure. The parallel GA implemented takes advantage of the CPU idle cycles of a computational grid, resulting in an application with a computational time of less than three minutes when processing pairs of standard intra-oral radiographs.

Categories and Subject Descriptors

G.1.6 [**Global Optimization**]; I.4 [**Image Processing**]: Applications; J.3 [**Life and Medical Sciences**]: Health

General Terms

Design, algorithms

Keywords

Genetic algorithms, image registration, distributed computing

1. INTRODUCTION

Digital subtraction radiography detects tissue mass changes by subtracting two digital radiographs. This method has shown to be very useful in early diagnosis of disease and follow-up examination [7, 10, 11]. When subtracting two radiographs taken over time, the image features which are coincident to both images can be removed and the small changes can be amplified to highlight their presence. For many years, digital subtraction radiography in dentistry has been used to qualitatively assess changes in radiographic density. Numerous authors have demonstrated the ability of this method to improve diagnostic performance for the detection of approximal dental caries [10], periapical pathology [11] and periodontal disease [12]. The use of digital subtraction radiography has also been shown to markedly increase the detection of destruction in the periodontal bone[21], as well as secondary caries detection [7]. A large variety of odontological diseases result in destruction of mineralized tissues, which are relatively small in the initial progression of the disease. A reliable detection and follow-up examination necessarily requires a precise alignment of the two images for the tissue changes to be detectable. Different approaches have been proposed for correcting such geometrical distortions. It goes from manual correction [28], to different devices used to ensure a consistent geometric projection which can be reliably reproduced over time [17]. However, in daily clinical practice, clinicians do not count with devices for adequate patient fixation, a drawback that has not allowed the application of this method to the series of routine examinations needed for progression estimation of lesions or treatments. In fact, since most clinicians do not pay attention to this issue, radiographic examinations generally produce strong geometrical distortions which makes it inappropriate to apply conventional correction approaches. Under these circumstances, standard numerical techniques for extrema searching in a parameter space like the Powell's method or the Downhill Simplex method [19] can yield irrelevant results.

In this paper, an entirely automatic method is proposed for spatial radiographic alignment in those cases where a considerable amount of distortion is present. The process starts by selecting one of the two images as the reference while the other is considered the floating image. Afterward, illumination differences are eliminated by means of an equalization algorithm explained below. Consecutive affine transformations are then performed on the floating image and the transformed image is compared to the reference using the correlation ratio as the similarity measure. An adaptive GA is used in order to find the transformation that produces the best match. The process is robust, reliable and reproducible on the test group of images.

2. IMAGE REGISTRATION PROBLEM

Conventional registration approaches have been successfully used in those situations where the patient's head has been appropriately fixated, therefore producing images with little distortions [24]. However, anatomical variations either from patient to patient or for the same patient in two

GECCO'05, June 25–29, 2005, Washington, DC, USA.

different moments, have been a major inconvenient for radiographic subtraction to become an applicable method in routine evaluations. Our problem can be therefore defined as a multi-parametric search in a highly irregular space of possible transformations, for which conventional approaches have a high probability of remain trapped in local extrema.

2.1 Parametric transformations

Small tissue deformations are conveniently modeled using affine or projective transformations. The affine transformation implemented in this analysis is defined as $T(x) = SRx + t$, where S is the scale matrix, R the rotation matrix and t the displacement vector.

2.2 Similarity measure

Mutual information measure[19], successfully applied to multimodal image registration[19, 27], assumes only statistical dependence between image intensities. It treats intensity values in a purely qualitative way, without considering any correlation or spatial information conveyed by nearby intensities. Mutual information tries to reduce entropy and this can be observed as a trend to form intensity clusters in the joint histogram. In our case, since we are dealing with monomodal images of natural tissue, the mutual information measure is under-constrained and we can assume a functional correlation. The concept of functional dependence, fundamental in statistics, provided us with the framework for the computation of similarity between the two images. To use this concept we consider images as random variables and interpret an image histogram as a probability density function. Furthermore, we consider the 2D histogram of a pair of images as their joint probability density function[23]. Thus when a pixel is randomly selected from an image X having N pixels, the probability of getting an intensity i is proportional to the number of pixels, N_i, in X having intensity i, i.e.,

$$P(i) = \frac{N_i}{N}. \tag{1}$$

In order to define the joint probability density function of an image pair we consider two images (X, Y) and a spatial transformation T that maps the set of pixels of Y, Ω_y, to the the set of pixels of X, Ω_x. As we are working with digitized radiographs, we can also assume that images X and Y take their intensity values from a known finite set $\mathcal{A} = \{0, ..., 255\}$:

$$X : \Omega_x \to \mathcal{A}, \quad Y : \Omega_y \to \mathcal{A}.$$

Now, by applying transformation T to image Y, a new mapping is defined from the transformed positions of Y to $\mathcal{A}$:

$$Y_T : T(\Omega_y) \to \mathcal{A}$$

$$\omega \mapsto Y[T^{-1}(\omega)].$$

We now have to find the intensities that a given point of $T(\Omega_y)$ simultaneously takes in X and Y_T. Since we are dealing with continuous spatial transformations, points of the grid $T(\Omega_y)$ do not, in general, transform to points of the grid Ω_x. So in order to define the joint probability density function of the images, we used the interpolation approach explained below, discarding the points of $T(\Omega_y)$ that do not have eight neighbors in Ω_x. If we denote by $T(\Omega_y)^*$ the subset of accepted points and by $\widetilde{X}$ the interpolation of X, we can define the image pair as the following couple:

$$Z_T : T(\Omega_y)^* \to \mathcal{A}^2$$

$$\omega \mapsto \left(\widetilde{X}(\omega), Y[T^{-1}(\omega)]\right),$$

and, in a similar way as we did for a single image in (1), their joint probability density function as:

$$P_T(i,j) = \frac{Card\,\{x | Z_T(x) = (i,j)\}}{Card\ T(\Omega_y)^*}. \tag{2}$$

On the other hand, the total variance theorem presented in [23]:

$$Var(Y) = Var[E(Y|X)] + E_X[Var(Y|X = x)], \tag{3}$$

expresses the fact that the variance can be decomposed as a sum of two energy terms: a first term $Var[E(Y|X)]$ that is the variance of the conditional expectation and measures the part of Y which is predicted by X, and a second term $E_X[Var(Y|X = x)]$ which is the conditional variance and stands for the part of Y which is functionally independent of X.

Now based on the previous equation, that can be seen as an energy conservation equation, we can define the *correlation ratio* as the measure of the functional dependence between two random variables:

$$\eta(Y|X) = \frac{Var[E(Y|X)]}{Var(Y)}.$$

The correlation ratio takes on values between 0 and 1, where a value near 1 indicates high functional dependence. Then, for a given transformation T, in order to compute $\eta(Y_T|X)$ we can use the following equation:

$$1 - \eta(Y_T|X) = \frac{E_X(Var(Y_T|X = x))]}{Var(Y_T)},$$

that by means of (2) and (3) can be expressed as:

$$1 - \eta(Y_T|X) = \frac{1}{\sigma^2} \sum_i \sigma_i^2\ P_{x,T}(i),$$

where:

$$\sigma^2 = \sum_j j^2\ P_y(j) - m^2, \quad m = \sum_j j\ P_y(j),$$

$$\sigma_i^2 = \frac{1}{P_x(i)} \sum_j j^2\ P(i,j) - m_i^2, \quad m_i = \frac{1}{P_x(i)} \sum_j j\ P(i,j).$$

The correlation ratio just discussed, measures the similarity between two images and is assumed to be maximal when the images are correctly aligned, thus will be used in our GA as the fitness value of the individuals.

2.3 Optimization problem

The problem we face is to find the optimal transformation that maximizes the correlation ratio between the pair of images. Therefore, the parameters to be found are the scale factor, the rotation angle and the horizontal and vertical translations.

3. PROPOSED APPROACH

3.1 Interpolation approach

In terms of linear interpolation, the reconstructed signal is obtained by convolution of the discrete signal (defined as a sum of Dirac functions) with a convenient selected kernel. We used spline interpolation [26] due to its accuracy and acceptable computing speed. Spline interpolation of order n is uniquely characterized in terms of a B-spline expansion:

$$s(x) = \sum_{\kappa \epsilon Z}^{\infty} c(\kappa)\beta^n(x-\kappa),$$

which involves integer shifts of the central B-spline. The parameters of the spline are the coefficients $c(\kappa)$. In the case of images with regular grids, they are calculated at the beginning of the procedure by recursive filtering. A three order approximation was used in the present work.

3.2 Search strategy

Genetic Algorithms are based on adaptive stochastic random search [13] simulating the natural selection process where only the fittest individuals survive. Despite their computational cost, genetic algorithms have been chosen over standard numerical methods because of their strong immunity to local extrema, their intrinsic parallelism and robustness, as well as their ability to cope with large and irregular search spaces. A good and diverse set of examples is presented in [2]. Multiple successful applications of GAs to image registration can be found in the literature [4, 16, 15], using monomodal and multi-modal images, 2D and 3D registration, in both sequential and parallel versions. However, references about the use of GAs to the specific case of subtraction radiography is limited to a very few cases (see for example [1]). Upon reviewing the most relevant works in this area, it can be concluded that the most crucial aspects refer to the coding scheme and the design of the fitness function. All seem to agree that for this kind of application, real-number encoding performs better than both binary and Gray encoding.

Accordingly, our genome has been coded as four floating point numbers representing the parameters used in the affine transformation [Fig. 1]. The initial population is created by applying random mutations over an individual that is either the null transformation or the center of mass transformation. The fitness of an individual, indicating the similarity between the transformed image and the reference image, is computed using the correlation ratio previously analyzed. Fit candidates, selected by tournament, are used for crossover in order to produce a new population.

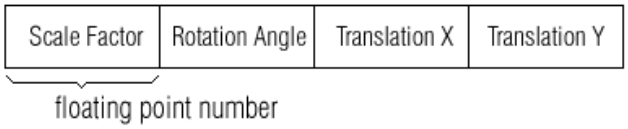

Figure 1: Real number encoding of the genome that represents a possible solution.

Crossover is performed applying a variation of the averaging crossover operator suggested by Davis in [5]. The genes of the offspring's chromosome are the result of a convex interpolation of the genes of the two mates selected from the population:

$$x_i = p_i * x1_i + (1 - p_i) * x2_i$$

$$p_i \in U(0, 1).$$

A mutation operator is applied to guarantee that the probability of searching a particular subspace of the problem space is never zero [3]. This prevents the algorithm from becoming trapped in local extrema [14, 9]. The mutation operator used, known as real number creep, sweeps the individual adding or subtracting a Gaussian distributed random noise to each parameter [5]. The creep operator implements a variation of neighborhood search by looking in the neighborhood of a good solution to see if better solutions exist.

Each new generation is then evaluated looking for a solution better than the best obtained so far. If a better solution is not found, the process is repeated in an inner loop reducing the search range for each iteration, until a better offspring is generated. Otherwise, if a maximum number of iterations is reached, the algorithm stops.

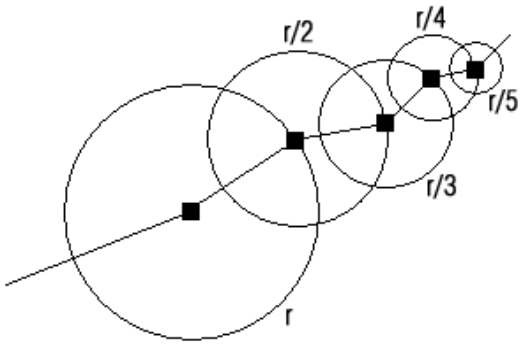

Figure 2: Search range is reduced linearly in each step of the inner loop.

3.3 Algorithm parallelization

The evaluation of the fitness function consists of applying an affine transformation and then computing of the corresponding correlation ratio. This computational intensive operation is required for each individual of the population. Since the operation can be computed independently for each individual, this part of the algorithm was parallelized and executed on a computational grid based on the JavaSpaces[1] computing model, using the well known replicated-worker pattern[8]. The grid is composed of forty general purpose workstations, with 1GHz processors and memory ranging from 256 to 512 Mbytes. Source code of the GA implemented and additional documentation about the computational grid is available at the unGrid Project site (`http://ungrid.unal.edu.co/telemedicine`).

4. ALGORITHM VALIDATION

To validate the correctness of the GA implemented, two sets of experiments were conducted. In both cases, the

[1]Java and JavaSpaces are trademarks of Sun Microsystems, Inc.

implemented GA was compared to a standard numerical method, the Downhill Simplex method due to Nelder and Mead[22]. This method was chosen because of its ease of implementation and because, amid the standard numerical optimization methods, it is the least sensitive to initial conditions. Firstly, a series of synthetic images was created by applying a set of known transformations to ten reference radiographs. Then the transformed images were registered to the original ones to verify the ability of each algorithm to find the values used in the transformation. In the second set of experiments the algorithms were evaluated with pairs of images obtained from real radiographs.

4.1 Synthetic transformation experiments

4.1.1 Experimental setup

The set of synthetic images was created by applying the transformations shown in Table 1, using a reliable image processing program. The algorithms were executed ten times for each pair of reference and synthetic image. The GA was executed on the computational grid while the Downhill Simplex implementation was executed on a single machine of the same grid.

	Transformation Applied			
	Rotation Angle	Scale Factor	T_x	T_y
1	1°	0.8	10	10
2	1°	0.8	100	100
3	1°	1.2	10	10
4	1°	1.2	100	100
5	30°	0.8	10	10
6	30°	0.8	100	100
7	30°	1.2	10	10
8	30°	1.2	100	100

Table 1: Some combinations of rotation, scaling and translation applied to the set of synthetic images.

4.1.2 Results and discussion

The transformation values and correlation ratio obtained by the Genetic Algorithm and the Downhill Simplex method, are presented in Table 2 and Table 3, respectively.

	Values found by GA					
	R	S	T_x	T_y	CR	Error%
1	1.016	0.791	9.426	9.897	0.922	2.7
2	1.115	0.798	96.667	98.034	0.884	6.8
3	0.984	1.190	9.972	10.267	0.936	1.3
4	1.230	1.177	94.564	95.996	0.895	8.6
5	29.794	0.797	9.196	9.9105	0.939	2.5
6	29.653	0.822	101.326	91.455	0.872	3.4
7	29.602	1.148	10.802	9.027	0.820	5.9
8	28.749	1.065	96.669	75.906	0.740	10.7

Table 2: Transformation values found by the Genetic Algorithm.

	Values found by DS					
	R	S	T_x	T_y	CR	Error%
1	1.035	0.723	8.547	8.782	0.719	10.0
2	1.215	0.618	85.378	116.802	0.630	18.9
3	1.117	0.975	7.742	8.754	0.569	16.4
4	1.230	0.912	78.781	72.349	0.536	24.0
5	26.127	0.607	13.396	8.910	0.576	20.5
6	21.653	0.522	111.873	127.572	0.589	25.5
7	24.367	0.985	14.431	8.535	0.522	23.9
8	19.756	0.769	111.304	123.761	0.556	26.3

Table 3: Transformation values found by the Downhill Simplex method.

Where the accuracy error was computed as:

$$E = 100 * \sum_{i}^{4} (ov_i - ev_i)/ev_i,$$

where ov represents the output value and ev the expected value.

From these results, it can be concluded that for transformations in the expected range, the GA outperforms the Downhill Simplex and provides clinically acceptable registration accuracy.

4.2 Real images experiments

4.2.1 Image Acquisition

Ten intra-oral radiograph pairs, taken at different occasions, were randomly selected from an unrelated study of periodontal therapy. No film holders or any other fixation device were mechanically coupled to the cone of the x-ray machine. Radiographs were digitized in a HP 3570 scanner using a transparent material adapter at a resolution of 600×600 DPI, producing 724×930 pixel images.

4.2.2 Preprocessing

Even though acquisition conditions are standardized as much as possible, illumination differences are inevitable. Thus, the histogram of the floating image is equalized by using the reference image luminances [25]. This transformation first computes the histogram of each image and then luminances are homogeneously distributed in the floating image according to the levels found in the reference image.

4.2.3 Experimental setup

The properties compared were accuracy, in terms of the similarity measure obtained, and efficiency, in terms of execution time and use of resources. Both algorithms were coded in Java and use the same routines to compute the correlation ratio between the transformed and reference image. The GA was executed on a computational grid while the Downhill Simplex implementation was executed on a single machine of the same grid.

4.2.4 Results and discussion

A summary of the results obtained is presented in Table 4:

It is worth noting that the Downhill Simplex method appeared to be very sensitive to the initial parameters and not always converged to the global optimum. While in some

Property	Simplex	GA
Average Correlation Ratio	0.587	0.876
Average Execution Time (secs)	42	171
Number of CPUs	1	40

Table 4: Simplex-GA comparison

executions it obtained better results than the GA, in other executions it produced meaningless values and this is reflected in the low overall accuracy shown in Table4. It is also important to note that the computational grid used to run the GA, only uses the free CPU cycles of the computers that comprise it.

Fig. 3 shows a pair of radiographs to be subtracted (top row). The bottom row displays subtraction without geometric correction on the left and with correction on the right. Null intensity level is shifted to 128 in order to make tissue changes easily observed.

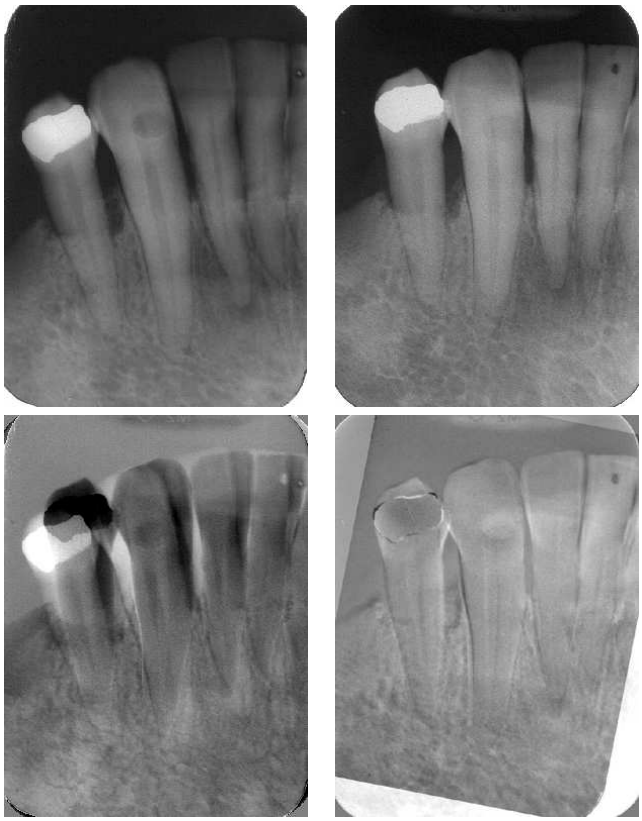

Figure 3: The upper row shows the two images to subtract. Bottom row shows the subtracted images: left without geometrical correction and right after automatic correction.

In this particular example it can be appreciated that the match is precise enough to make objective measurements despite the fact that in the second radiograph, the fifth tooth (from left to right) is nearly hidden. The small spot, likely an artifact, that appears in both images is observed in the resultant image in white indicating that a pure difference is present. In this image it can also be observed that a difference appears at the root of the third tooth which corresponds to new tissue developed after treatment. These changes are impossible to be observed at the raw difference image (bottom left). Similarly, in this image the bone pattern is blurred and impossible to be unrecognizable, while in the resultant image the trabecular bone pattern is clear. For the entire set of test images, matching has been visually assessed by two experts in the domain who have judged that the alignment is sufficiently accurate to get objective measurements, while maintaining acceptable computation times.

4.3 GA parameter analysis

A number of 4580 experiments were performed in order to guarantee a complete analysis of the parameter space. An experiment is the execution of the algorithm with a particular set of images and parameters, i.e. population size, tournament size and genetic operators probabilities. In this task the grid became an essential tool and allowed us to achieve a second level of parallelism.

The first analysis was conducted to determine two basic parameters of the GA: population size and selection scheme used to choose the parents for crossover.

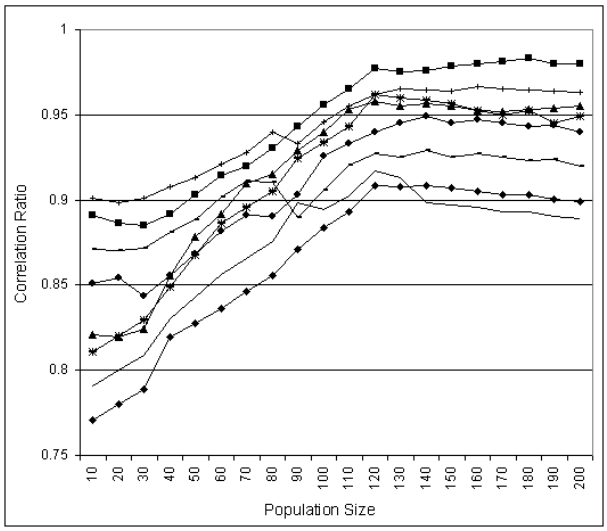

Figure 4: Most appropriate population size averaged 120 in the ten radiographs pairs subtracted. Above this value, the process slows down and no better results are obtained.

Two common selection options are tournament selection and elitism. In tournament selection of size N, N individuals are selected at random and the fittest is chosen. Elitism is a particular case of tournament selection where the size of the tournament equals the size of the population, so the best individual is always preserved. Fig. 4 shows the experiments performed to find the most appropriate population size.

Fig. 5 shows that for this particular problem, tournament selection is the best option for selecting the parents for a new generation. The other parameters analyzed were the crossover and mutation probabilities. The combination of probabilities that yielded the best results were 0.65 and 0.21 respectively.

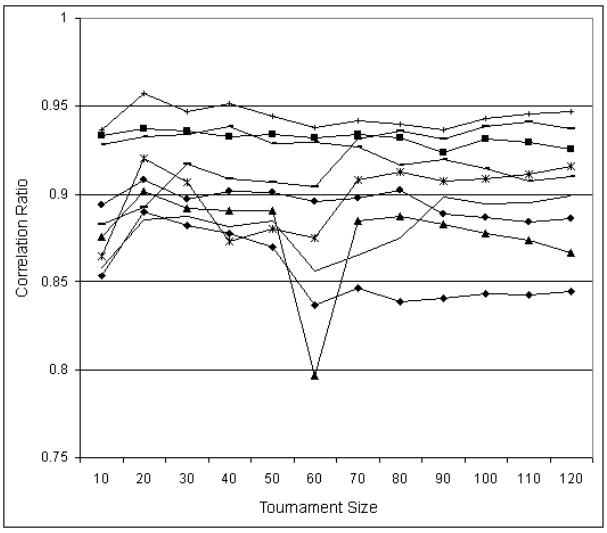

Figure 5: Best selection scheme was found to be tournament of size 20 in average.

The average time to compute an experiment with a population of 120 individuals is about 48 minutes if run on a single machine. This time was reduced to less than three minutes using the parallel implementation of the GA. The speedup obtained by parallelizing the algorithm is near 17 and can be explained by examining the timing profile of the sequential GA, where about 95 percent of the time is spent on applying the affine transformation and computing the correlation ratio (eighty and fifteen percent, respectively).

5. CONCLUSION

An entirely automatic and fast method for strong geometric correction in subtraction radiography is proposed. The method uses the correlation ratio as the similarity measure and a GA strategy for searching an optimal transformation. Preliminary results show the consistency of the technique in ten different cases of clinical subtraction radiography, randomly selected from a set of one hundred studies. It must be stressed that in these studies no attention was paid to the fixation protocol and indeed we used no fixation at all. For although fixation methods based on anatomical considerations such as repair points or implementation of routine angles of the x-ray cone can help obtain similar positions of the radiographs, the chance of variation in angles is strong enough to produce radiographs whose main planes result in very large geometrical distortions. Under these conditions, the GA used, although costly computationally, showed good and fast convergence toward a satisfactory solution, evaluated by two different experts in the domain. Furthermore, the computational burden was lessened considerably by parallel implementation. The fact that the tournament selection scheme proved to be the best approach, shows that diversity is a necessary condition when using evolutionary algorithms. Finally, we can conclude that the registration method turned out to be a useful and objective measurement of the differences between pairs of radiographs. Further clinical studies will be conducted in order to evaluate our approach in larger samples and more complex cases.

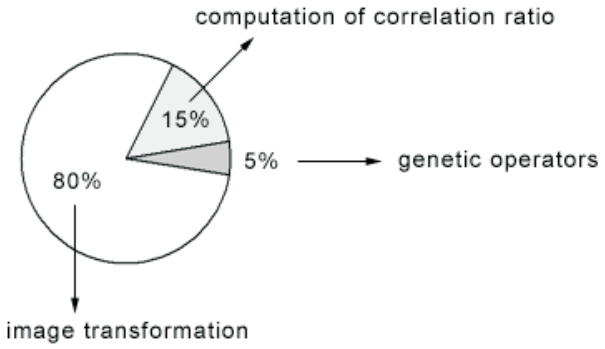

Figure 6: Timing profile of the sequential GA.

6. REFERENCES

[1] M. R. Benbrahim, R. Benslimane and El. Aalloula "Automatic retiming method based on genetic algorithm for the detection and the follow-up of dental lesions", *Electronic Journal Technical Acoustics.*, 12, 2004

[2] L. Chambers, "The Practical Handbook of Genetic Algorithms: Applications", *Second Edition, Chapman and Hall/CRC Press, Inc.*, 2000

[3] A. Chipperfield and P. Fleming, "Parallel Genetic Algorithms", *Parallel and Distributed Computing Handbook by A. Y. H. Zomaya*, McGraw-Hill, 1996, pp. 1118–1143

[4] A. D. J. Cross, R. C. Wilson, and E. R. Hancock, "Genetic search for structural matching", *Computer vision - ECCV, Vol. 1064 of Lecture notes in Computer Science*, 1996, pp. 514-525

[5] L. Davis, "Handbook of genetic algorithms", *Van Nostrand Reinhold*, 1991, pp. 435–440

[6] J. E. Duckworth, P. F. Judy, J. M. Goodson and S. S. Socransky, "A method for the geometric and densitometric standardization of intraoral radiographs", *Journal of Periodontal Research*, 54, 1983, pp. 435–440

[7] E. C. Ekberg, A. Petersson and M. Nilner, "An evaluation of digital subtraction radiography for assessment of changes in position of the mandibular condyle", *Dentomaxillofacial Radiology*, 27, 1998, pp. 230–235

[8] E. Freeman, S. Hupfer and K. Arnold, "JavaSpaces(tm) Principles, Patterns, and Practice", *Pearson Education*, 1999, pp. 153–164

[9] D. A. Goldberg, "Genetic Algorithms in Search, Optimization and Machine Learning", *Reading, Mass. Addison-Wesley*, 1989, pp. 305–324

[10] H. G. Grondahl, K. Grondahl, T. Okano and R. L. Webber, "Statistical contrast enhancement of subtraction images for radiographic caries diagnosis", *Oral Surgery*, 53, 1982, pp. 219–223

[11] H. Grondahl, K. Grondahl and R. Webber, "A digital subtraction technique for dental radiography", *Oral Surgery*, 55, 1983, pp. 96–102

[12] H. Grondahl and K. Grondahl, "Subtraction radiography for the diagnosis of periodontal bone lesions", *Oral Surgery*, 55, 1983, pp. 208–213

[13] J. H. Holland, "Adaptation in Natural and Artificial Systems", *University of Michigan Press, Ann Arbor*, 1975, pp. 329–346

[14] P. Husband, "Genetic Algorithms in Optimization and Adaptation", *Advances in Parallel Algorithms Kronsjo and Shumsheruddin ed.*, 1990, pp. 227–276

[15] J. Jacq and C. Roux, "Registration of non-segmented images using a genetic algorithm", *Computer vision, virtual reality, and robotics in medicine, Vol. 905 of Lecture notes in Computer Science*, 1995, pp. 205-211

[16] B. Laksanapanai, W. Withayachumnankul, C. Pintavirooj

and P.Tosranon, "Acceleration of Genetic Algorithm with Parallel Processing with Application in Medical Image Registration", *Lecture notes of the 13th International Conference in Central Europe on Computer Graphics, Visualization and Computer Vision*, University of West Bohemia, 2005

[17] J. B. Ludlow and C. P. Peleaux, "Comparison of stent versus laser-and cephalostat-aligned periapical film-positioning techniques for use in digital subtraction radiography", *Oral Surgery*, 77(2), 1994, pp. 208–215

[18] F. Maes, A. Collignon, D. Vandermeulen, G. Marchal, and P. Suetens. "Multimodality Image Registration by Maximization of Mutual Information", *IEEE Transactions on Medical Imaging*, 1997, pp. 16(2):187-198.

[19] J. B. A. Maintz and M. A. Viergever, "An Overview of Medical Image Registration Methods", *Symposium of the Belgian hospital physicists association (SBPH/BVZF)*, 12, 1996-1997, pp. V:1-22

[20] Z. Michalewicz, "Genetic Algorithms + Data Structures = Evolution Programs", *AI Series, Springer-Verlag, New York*, 1994

[21] P. V. Nummikoski, T. S. Martinez, S. R. Matteson, W. D. McDavid and S. B. Dove, "Digital subtraction radiography in artificial recurrent caries detection", *Dentomaxillofacial Radiology*, 29(2), 1992, pp. 59–64

[22] W. H. Press, S. A. Teulkolsky, W. T. Vetterling and B. P. Flannery, "Numerical Recipes in C, The Art of Scientific Computing", *Cambridge University Press, Second Edition*, 2002, pp. 408–412

[23] A. Roche, G. Malandain, X. Pennec and N. Ayache, "Multimodal Image Registration by Maximization of the Correlation Ratio", *INRIA Sophia Antipolis, Rapport de recherche n^o 3378*, August, 1998

[24] E. Romero, W. J. Sarmiento and A. Lozano, "An Automatic Algorithm for Geometric Correction in Subtraction Radiography", *IEEE International Workshop on BioMedical Circuits and Systems*, 2004, Singapure

[25] U. E. Ruttimann, R. L. Webber and E. Schmidt, "A robust digital method for film contrast correction in subtraction radiography", *Journal of Periodontal Research*, 21, 1986, pp. 486–495

[26] M. Unser, "A perfect fit for image signal processing", *IEEE Signal Processing Magazine*, 16, 1999, pp. 22–38

[27] P. Viola, "Alignment by Maximization of Mutual Information", *PhD thesis, M.I.T, Artificial Intelligence Laboratory*, 1995.

[28] A. Wenzel, "Effect of manual compared with reference point superimposition on image quality in digital subtraction radiography", *Dentomaxillofacial Radiology*, 18, 1989, pp. 145–150